Ultrafast spectroscopy and control of correlated quantum materials

By

Bryan T. Fichera

B.S., University of Pennsylvania (2017)

Submitted to the Department of Physics
in partial fulfillment of the requirements for the degree of

Doctor of Philosophy

at the

MASSACHUSETTS INSTUTITE OF TECHNOLOGY

May 2024

Authored by: Bryan T. Fichera
Department of Physics
May?, 2024

Certified by: Nuh Gedik
Donner Professor of Physics, Thesis supervisor

Accepted by: ?
? Professor of ?
? Chair of ?

Abstract

Lorem ipsum dolor sit amet, consectetuer adipiscing elit. Etiam lobortis facilisis sem. Nullam nec mi et neque pharetra sollicitudin. Praesent imperdiet mi nec ante. Donec ullamcorper, felis non sodales commodo, lectus velit ultrices augue, a dignissim nibh lectus placerat pede. Vivamus nunc nunc, molestie ut, ultricies vel, semper in, velit. Ut porttitor. Praesent in sapien. Lorem ipsum dolor sit amet, consectetuer adipiscing elit. Duis fringilla tristique neque. Sed interdum libero ut metus. Pellentesque placerat. Nam rutrum augue a leo. Morbi sed elit sit amet ante lobortis sollicitudin. Praesent blandit blandit mauris. Praesent lectus tellus, aliquet aliquam, luctus a, egestas a, turpis. Mauris lacinia lorem sit amet ipsum. Nunc quis urna dictum turpis accumsan semper.

Acknowledgements

Preface

The physics of solids is, to me, one of the most important and fundamental fields of modern science. This might seem, to some, a bit of a hot take. After all, by studying condensed matter physics, one learns next to nothing about, say, the formation of the stars and planets, or the origin of the universe. Nor does one learn about life, death, consciousness, disease, ethics, God, or any other question that perhaps puzzled humanity prior to about five hundred years ago. Certainly no one would argue that condensed matter physics is quite *useless*, given that nearly every device we interact with in modern life required some condensed matter physicist somewhere along the way to make one brilliant discovery or another – yet when the human mind starts to wander, and our thoughts turn to the metaphysical, we tend to look up, not down.

In my work I have taken a quite different view. Condensed matter physics, to me, is ultimately the study of how *truly boring* objects, when brought together in large quantites, *become* interesting, seemingly in spite of themselves. When electrons are put together in a lattice and allowed to interact slightly with the massive nuclei, at low enough temperatures they pair, the low-energy excitations become gapped, and current can flow for infinite times and with absolutely zero energy loss. Those same electrons, with some other set of interactions, may instead ionize (the opposite of pairing!) to create an electrically insulating state, whose low-energy excitation spectrum is nevertheless gapless and consisting of charge-neutral spin-$1/2$ particles. In all such cases, these systems exist in otherwise ordinary-looking rocks, fit in the palm of a hand[1], and are more or less indistinguishable from something you might find sticking into the bottom of your shoe.

While such systems may not tell us a lot[2] about the early universe, considering these and related problems lets us ask deep, fundamental questions about the world we live in – like, why is this thing a metal, but this thing is an insulator? What do those terms even mean? – that I don't think we would try to ask otherwise. To me, focusing our attention on

[1] Hopefully, gloved.

[2] This discussion is obviously intentionally reductive. In truth there is still quite a bit one can learn about, e.g. the early universe by studying condensed matter physics, see the review by Kibble *et al.*, Ref. 1.

these problems, despite their obviously terrestrial nature, is not a waste of time; rather, I think they remind us that even the most mundane aspects of the human experience involve a level of complexity far beyond what we are capable of understanding absent the pursuit of science.

Throughout the seven years of my Ph.D., I hope to have made a few contributions to this pursuit. As the title of this work implies, I have mainly focused on the application of ultrafast techniques to the study of correlated quantum materials, which I loosely define as those materials in which the interaction between particles is large enough so as to compete with the kinetic energy of those particles. It is in these materials that I think lies the true frontier of condensed matter physics; here, much of our basic intuition about non- or weakly-interacting theory fails, and more complicated notions of phase competition, phase separation, disorder, pairing, coherence, etc. are needed to property describe the relevant physics.

In my own view, and in the view of many scientists in this field [2], the main question for strongly correlated physics amounts to: "Given a correlated system with some defined combination of different interaction strengths, is there a general theory which allows us to predict the phase diagram of this system *a priori*?" Related of course are questions about the origins of high-T_c superconductivity, strange metallicity, quantum spin liquids, and other exotic phases that we find emerging from strongly interacting systems. Since such a theory does not currently exist, at least with the level of predictive power that I think most would find satisfactory, new advances in this field typically come directly from experiment. Ultrafast optics plays a special role in this regard, for reasons that I will explain in chapter 1.

Progress thus happens in this field somewhat unsystematically, with small pieces of the puzzle added at random, but not infrequenct, intervals. Usually it is either new techniques or new materials that are the driving force here. To this end, I have tried to pursue both directions in my Ph.D. Appearing also in chapter 1 is thus a description of the materials I studied the most during my thesis, two of them, $CuBr_2$ and $CaMn_2Bi_2$ I consider criminally understudied. On the technique side, almost all of the work presented in this thesis was done using time resolved second harmonic generation (tr-SHG), a relatively new, nonlinear optical technique which, at the most basic level, probes the point group assumed by the charge distribution function $\rho(\boldsymbol{x})$ at any given point in time. Sec-

ond harmonic generation (SHG) and tr-SHG are tricky techniques, with many pitfalls both practically and theoretically; chapter 2 and **??** are thus devoted to what I hope is a useful, if not fully compehensive, description of the technique. My hope is that these sections are useful not only for the new student trying to build their own setup or analyze their own SHG data, but also for people for whom SHG is not a focus but nevertheless want to learn about it in slightly more detail than one would get from a typical paper or review article. Some aspects of **??** are devoted to work that we did developing a new way to control the polarization of the light in a tr-SHG experiment using stepper motors.

What follows, then, is a description of the three main research works I contributed during my Ph.D.. The first, which I describe in **??**, involves work that I did during my second and third years on $1T$-TaS_2, a very interesting charge density wave (CDW) material that, among other things, undergoes a mirror symmetry breaking CDW transition at $350\ \mathrm{K}$ that shows up in the SHG as a sudden distortion of the flower pattern at that temperature. Since this transition breaks mirror symmetry, two energetically degenerate domains should be present, corresponding to two opposite planar chiralities; in this work, we showed that SHG could differentiate between these two domains (i.e. the flower pattern in either domain looks different).

The second and third works, which I describe in **????**, in contrast to the $1T$-TaS_2work, both involve taking the system out of equilibrium to study the dynamics. In $CaMn_2Bi_2$ (**??**), we discovered that photoexcitation causes the antiferromagnetic (AFM) order in that compound to reorient (relative to equilibrium) to a metastable state which is impossible to reach from the equilibrium state thermodynamically. Light is thus used to *control* the magnetic order in this material.

In $CuBr_2$ (**??**), light is not used to control the order parameter like in $CaMn_2Bi_2$, but it does excite coherent oscillations of the collective modes of the multiferroic order (electromagnons), whose frequency, amplitude, damping, etc. may be probed in tr-SHG as a function of temperature – a methodology referred to as ultrafast *spectroscopy*. In doing so, we found that one of these collective modes is actually quite special, as it is in fact the analogue of the Higgs mode of particle physics in the context of a multiferroic material.

I conclude with various remarks in **??**, as well as an appendix, in which I enumerate briefly all of the null-result experiments I performed

during my Ph.D., in the hopes that future scientists don't have to waste time on what we already know are fruitless pursuits. If you have any questions about this or any other section of this thesis, please do not hesitate to reach out via email.

Contents

List of Figures

List of Tables

Chapter One

Ultrafast optics in correlated electron systems

Chapter Two

Second harmonic generation: theory

2.1 Space groups, point groups, and Neumann's principle

The utility of SHG in studying condensed matter systems is derived from the following simple statement, attributed to Franz Neumann [3] and later Pierre Curie [4]:

Theorem 2.1.1 (Neumann's principle) *Let P_G be the symmetry group of a crystal structure and P_H the symmetry group of some physical property of that crystal. Then, P_G is a subgroup of P_H.*

There are a few things to digest here. Let us start by understanding the meaning of the phrase "symmetry group". For any given crystal, there exists some infinitely large set of operations G under which the crystal structure is symmetric. Each of these operations may be decomposed into two parts: a "point-preserving operation" R, corresponding to either the identity, rotation, inversion, mirror, or the product of mirror and rotation, followed by a translation by some vector $\boldsymbol{\tau}$:

$$G = \{(R|\boldsymbol{\tau})\} \tag{2.1}$$

where $(R|\boldsymbol{\tau})$ means "Perform R, then translate by $\boldsymbol{\tau}$". Clearly, the set G forms a group, since if both g_1 and $g_2 \in G$ leave the crystal structure

invariant, so does the product $g_1 g_2$, and so $g_1 g_2 \in G$. Thus, G is called the *space group* of the crystal. In three dimensions, there are 230 crystallographic space groups, which are tabulated in a number of places, most usefully Wikipedia [5].

For 73 of these groups, the translation parts of the $\boldsymbol{\tau}$'s in eq. (2.1) are only ever linear combinations of integer multiples of the lattice vectors $\boldsymbol{a}$, $\boldsymbol{b}$, and $\boldsymbol{c}$; these are called *symmorphic* space groups. The remaining 157 groups involve translations that are not integer multiples of the lattice vectors; these are one's screw axes and glide planes, and so these groups are called *asymmorphic*.

Importantly, the "physical properties" of theorem 2.1.1 refer to the truly macroscopic properties of the crystal, like its conductivity, dielectric, or pyroelectric tensors. Consider, for example, that in SHG, we are typically studying the sample at optical wavelengths, where the wavelength of light is three or four orders of magnitude larger than the lattice spacing. Clearly, then, these properties do not care whether the correct symmetry is $(R|\boldsymbol{\tau})$ or $(R|\boldsymbol{\tau} + \boldsymbol{a}/2)$. A more useful group, then, is the *point group* of the crystal

$$P_G = \{R \text{ s.t. } \exists\, \boldsymbol{\tau} \text{ s.t. } (R|\boldsymbol{\tau}) \in G\} \tag{2.2}$$

i.e., the point group is the set of point-preserving operations R for which R appears in G, regardless of whether you need to perform a translation with it. Once can show that P_G is also a group, and thus it is P_G which is involved in Neumann's principle for all intents and purposes[1].

The last ingredient that we need to understand theorem 2.1.1 is the concept of what is meant by "physical propery". The idea is that the response of the crystal $J_{i_1 i_2 \cdots i_n}$ (i.e., the current J_i, or the quadrupole moment Q_{ij}) is proportional to some field $F_{i'_1 i'_2 \cdots 1'_m}$ via some tensor χ:

$$J_{i_1 i_2 \cdots i_n} = \chi_{i_1 i_2 \cdots i_n i'_1 i'_2 \cdots i'_m} F_{i'_1 i'_2 \cdots 1'_m}. \tag{2.3}$$

For example, the conductivity σ_{ij} relates a current density J_i to an applied electric field E_j:

$$J_i = \sigma_{ij} E_j. \tag{2.4}$$

[1]Of course this breaks down when the wavelength of light is comparable to the lattice spacing; in that case you need to consider the full space group.

Likewise, the polarization P_i due to the pyroelectric effect is related to the a temperature difference ΔT by a tensor p_i:

$$P_i = p_i \Delta T. \tag{2.5}$$

The tensors σ_{ij}, p_i, and generally, $\chi_{i_1 i_2 \cdots 1_n i'_1 i'_2 \cdots i'_m}$ are commonly referred to as *matter tensors* [6], to emphasize the fact that they are the only part of the response equations that depend on the material. It should be noted that matter tensors generically come in two types: those that transform like a vector under inversion and those that transform like a pseudovector under inversion. You can tell which is which by applying inversion to either side of the response equation. For example, the tensor ϵ_{ij} relating the displacement field to the electric field

$$D_i = \epsilon_{ij} E_j \tag{2.6}$$

is a polar tensor, whereas the tensor χ_{ij}^{me} describing the magnetoelectric effect

$$M_i = \chi_{ij}^{me} E_j \tag{2.7}$$

is an axial tensor.

We are now ready to restate theorem 2.1.1 in a slightly more useful form, using the terminology we have developed about point groups and matter tensors:

Theorem 2.1.2 (Neumann's principle, restated) *Let P_G be the point group of a given crystal, and let χ be a matter tensor describing some response function of that crystal. Then, for all $g \in P_G$, we have*

$$g(\chi) = \chi. \tag{2.8}$$

Equation (2.8) can be more usefully expressed if we know the matrix R_{ij}^g corresponding to g. For example, if g is "threefold rotation about the z axis", we have

$$R_{ij}^g = \begin{pmatrix} -\frac{1}{2} & -\frac{\sqrt{3}}{2} & 0 \\ \frac{\sqrt{3}}{2} & -\frac{1}{2} & 0 \\ 0 & 0 & 1 \end{pmatrix}, \tag{2.9}$$

in which case one can show that eq. (2.8) reads

$$(\det R^g)^t R_{i_1 i'_1}^g R_{i_2 i'_2}^g \cdots R_{i_n i'_n}^g \chi_{i'_1 i'_2 \cdots i'_n} = \chi_{i_1 i_2 \cdots i_n}, \tag{2.10}$$

where t is 0 if χ is a polar tensor and 1 if χ is an axial tensor. Theorem 2.1.2 tells us that there is one copy of eq. (2.10) for each $g \in P_G$.

Apparently, each element $g \in P_G$ gives us a *constraint* on the numbers $\chi_{i_1 i_2 \cdots i_n}$, in that they have to satisfy eq. (2.10). This is a remarkably useful fact. Since different point groups enforce different constraints on χ, that means the *form* of χ (e.g. when written as a list of numbers) depends quite sensitively on the point group of the crystal we are studying. As an example, here is the dielectric permittivity tensor for crystals with the point group (in Schoenflies notation) C_2:

$$\epsilon_{ij} = \begin{pmatrix} a & 0 & e \\ 0 & b & 0 \\ e & 0 & c \end{pmatrix}_{ij} \tag{2.11}$$

versus in the point group D_{3d}:

$$\epsilon_{ij} = \begin{pmatrix} a & 0 & 0 \\ 0 & a & 0 \\ 0 & 0 & c \end{pmatrix}_{ij} . \tag{2.12}$$

Clearly, any *measurement* of ϵ_{ij} will be able to easily differentiate a crystal with point group C_2 from one with point group D_{3d}. This is the fundamental basis, then, for SHG. In SHG, we measure the tensor χ_{ijk} corresponding to the response equation[2]

$$P_i(2\omega) = \chi_{ijk} E_j(\omega) E_k(\omega); \tag{2.13}$$

the numbers χ_{ijk} thus tell us about the crystallographic point group we are measuring from.

There are a couple of advantages to measuring χ_{ijk} over any other matter tensor in a given system. For one thing, χ_{ijk} is a third rank tensor, which means it has a few more degrees of freedom to work with compared to ϵ_{ij}, and thus does a better job at uniquely specifying each point group. It also doesn't have *too many* degrees of freedom, so that most of the time your experiment will be able to tell you all of your tensor elements[3]. In addition, since we are typically doing SHG at optical

[2]This discussion is a bit simplified in the sense that there are actually *many* response functions which will give you light at 2ω; for a more detailed discussion, see section 2.2.

[3]Quadrupole SHG has this problem, see section 2.2.

wavelengths, the form of χ_{ijk} reflects the symmetry of the *charge distribution* $\rho(\boldsymbol{x})$, in contrast to e.g. x-ray diffraction, where the relevant tensors will tell instead you about the electron distribution, $n(\boldsymbol{x})$. This can be advantageous in cases where the long range order you are trying to study involves an ordering of the valence electrons but not the electrons in the cores of atoms. This is entirely the result of the fact that Neumann's principle, as expressed both in theorem 2.1.1 and theorem 2.1.2, tells us that the point group of our crystal is a *subgroup* of the point group we get from our measurement – the measurement can always be more symmetric than the crystal!

As another example of this fact, let us note that the response equation given by eq. (2.13) clearly has an additional symmetry $j \leftrightarrow k$, since the two copies of the electric field on the right hand side are equivalent. Obviously this is not a result of the material we are studying, it is simply a fact of doing SHG. Thus, in addition to the constraints given by Neumann's principle and eq. (2.10), we have the additional constraint

$$\chi_{ijk} = \chi_{ikj} \forall i, j, k. \tag{2.14}$$

This is known as *particularization* [7].

2.2 A classical understanding of SHG

In the last section we considered the SHG response function given by eq. (2.13). Where does this relationship come from, and how is $P(2\omega)$ eventually measured? Our starting point in the classical treatment will be the inhomogenous electromagnetic wave equation

$$\left(\nabla^2 - \frac{1}{c^2}\frac{\partial^2}{\partial t^2}\right) E_i(\boldsymbol{x}, t) = S_i(\boldsymbol{x}, t), \tag{2.15}$$

which we understand as defining the field $E_i(\boldsymbol{x}, t)$ radiated by the source term $S_i(\boldsymbol{x}, t)$, which is induced by the incident field. To lowest order in a multipole expansion, $S_i(\boldsymbol{x}, t)$ is given by [**?**, 8]

$$\mu_0 \frac{\partial^2 P_i(\boldsymbol{x}, t)}{\partial t^2} + \mu_0 \left(\epsilon_{ijk} \nabla_j \frac{\partial M_k(\boldsymbol{x}, t)}{\partial t}\right) - \mu_0 \left(\nabla_j \frac{\partial^2 Q_{ij}(\boldsymbol{x}, t)}{\partial t^2}\right) \tag{2.16}$$

where $P_i(\boldsymbol{x}, t)$, $M_i(\boldsymbol{x}, t)$, and $Q_{ij}(\boldsymbol{x}, t)$ are the induced electric dipole, magnetic dipole, and electric quadrupole densities, and ϵ_{ijk} is the Levi-Civita tensor.

If the incident electric field is small, then the terms $P_i(\boldsymbol{x},t)$, $M_i(\boldsymbol{x},t)$, and $Q_{ij}(\boldsymbol{x},t)$ are linear functions of that electric field. However, for larger incident fields (such as those generated by pulsed lasers), they may be more generally written as a taylor series:

$$P_i = \chi^{ee}_{ij}E_j + \chi^{em}_{ij}H_j + \chi^{eee}_{ijk}E_jE_k + \chi^{eem}_{ijk}E_jH_k + \cdots \tag{2.17}$$

$$M_i = \chi^{me}_{ij}E_j + \chi^{mm}_{ij}H_j + \chi^{mee}_{ijk}E_jE_k + \chi^{mem}_{ijk}E_jH_k + \cdots \tag{2.18}$$

$$Q_{ij} = \chi^{qe}_{ijk}E_k + \chi^{qm}_{ijk}H_k + \chi^{qee}_{ijkl}E_kE_l + \chi^{qem}_{ijkl}E_kH_l + \cdots \tag{2.19}$$

where we have suppressed the arguments $\boldsymbol{x}$ and t for brevity.

Assuming the incident field is monochromatic,

$$E_i(\boldsymbol{x},t) = E_i(\omega)e^{i(\boldsymbol{k}\cdot\boldsymbol{x}-\omega t)} + \text{c.c.} \tag{2.20}$$

$$H_i(\boldsymbol{x},t) = H_i(\omega)e^{i(\boldsymbol{k}\cdot\boldsymbol{x}-\omega t)} + \text{c.c.} \tag{2.21}$$

the induced sources are also monochromatic, and (keeping only terms proportional to $e^{i2\omega t}$) we thus get

$$P_i(2\omega) = \chi^{eee}_{ijk}E_j(\omega)E_k(\omega) + \chi^{eem}_{ijk}E_j(\omega)H_k(\omega) \tag{2.22}$$

$$M_i(2\omega) = \chi^{mee}_{ijk}E_j(\omega)E_k(\omega) + \chi^{mem}_{ijk}E_j(\omega)H_k(\omega) \tag{2.23}$$

$$Q_{ij}(2\omega) = \chi^{qee}_{ijkl}E_k(\omega)E_l(\omega) + \chi^{qem}_{ijkl}E_k(\omega)H_l(\omega). \tag{2.24}$$

Since eq. (2.15) is linear, the electric field radiated by $S_i(\boldsymbol{x},t)$ is simply proportional to it. In the limit where the first term of eq. (2.22) dominates, the intensity measured at our detector thus satisfies

$$I(2\omega) \propto |\hat{e}^{\text{out}}_i \chi^{eee}_{ijk} \hat{e}^{\text{in}}_j \hat{e}^{\text{in}}_k|^2, \tag{2.25}$$

where $\hat{\boldsymbol{e}}^{\text{in}}$ and $\hat{\boldsymbol{e}}^{\text{out}}$ are unit vectors in the direction of the incoming and measured electric fields[4]. χ^{eee}_{ijk} does typically dominate when inversion symmetry is broken, but if not, you have to consider all of the terms in eqs. (2.22) to (2.24). Actually, each of these terms needs to be considered twice, since there is both a surface contribution and a bulk contribution[5]. In my experience, the heirarchy of contributions (from most to least important, and assuming everything is allowed by symmetry) is typically:

[4]Usually there are polarizers in the experiment which define these directions.

[5]The space group which constrains the surface contributions is the bulk space group less the operations which involve some change in the z coordinate.

1. Bulk electric dipole

2. Surface electric dipole, bulk electric quadrupole, and bulk magnetic dipole, at the same order[6]

3. Everything else

I've never seen anything outside of items 1 and 2, but in rare cases an electronic resonance may cause an enhancement in one of the other contributions [9].

Let us take a moment now to emphasize the following extremely common misconception about SHG: just because you see SHG in your experiment, that does not mean that inversion symmetry is broken in your material! It also does not mean that your material is a ferroelectric, or really that there's anything special at all about your material, at least before you've done any further analysis. Similarly, if you *don't* see SHG, that doesn't mean inversion symmetry is preserved, either. I have repeatedly seen large electric quadrupole SHG show up in materials with inversion symmetry, while materials which definitely break inversion symmetry have absolutely zero SHG observable in the experiment. The reason for this is ultimately due to resonance, a topic which I will discuss in section 2.3, but I mention it here because it is truly quite common in the literature and it is surely a mistake worth avoiding. You are "allowed" to say your material breaks inversion symmetry only if there is no other contribution in eqs. (2.22) to (2.24) which fits your data, and you are basically never allowed to say that your material preserves inversion symmetry when there is no SHG (a fact that should be obvious on a careful reading of theorem 2.1.1).

2.3 SHG in quantum mechanics

The description of SHG in the previous section is probably the most useful for understanding SHG from an "optics" perspective, but it gives little

[6]Somehow the bulk electric quadrupole and magnetic dipole contributions have been labelled "exotic" by some in the community, but that has not been my experience. If I had to guess, almost half of the materials I have measured with inversion symmetry show electric quadrupole SHG.

insight into the true microscopic origin of the SHG intensity. The quantum description, on the other hand, will tell you exactly where the SHG is coming from microscopically, but only if you have access to the eigenfunctions $|\psi\rangle$ of your hamiltonian – it is of little use otherwise. Nevertheless, we can still gain intuition about the dependence of our SHG intensity on the frequency of the light in the quantum picture, which will be useful for clearing up a whole other slew of misconceptions that have somehow made their way into the SHG literature. This treatment closely follows that of Ref. 10.

The starting point is to describe the system under study as a statistical ensemble specified by a Hamiltonian

$$H = H_0 + \lambda V \tag{2.26}$$

and a density matrix

$$\rho(t) = \sum_i p_i(t) \, |\psi_i(t)\rangle \, \langle\psi_i(t)| \tag{2.27}$$

where the $p_i(t)$'s specify the classical probability of the system being in state i at time t, and the $|\psi_i\rangle$'s are wavefunctions given by

$$|\psi_i(t)\rangle = \sum_n c_n^i(t) \, |n\rangle \tag{2.28}$$

for some $\{c_n^i(t)\}$, where

$$H_0 \, |n\rangle = E_n \, |n\rangle \tag{2.29}$$

for all n. In the presence of damping, the elements

$$\rho_{nm} = \langle\psi_n| \, \rho \, |\psi_m\rangle \tag{2.30}$$

of ρ satisfy the differential equation

$$\dot{\rho_{nm}} = \frac{1}{i\hbar}[H, \rho]_{nm} - \gamma_{nm}(\rho_{nm} - \rho_{nm}^{(\mathrm{eq})}), \tag{2.31}$$

where γ_{nm} is a matrix of (phenomenological) damping parameters[7], and $\rho_{nm}^{(\mathrm{eq})}$ is the density matrix corresponding to the equilibrium steady state of the system.

[7] This is just one choice of $p_i(t)$.

We consider the case where V may be treated as a perturbation on top of H_0, i.e. where λ is small. In this case, eq. (2.31) can be written

$$\dot{\rho}_{nm} = -i\omega_{nm}\rho_{nm} + \frac{1}{i\hbar}\sum_k \lambda(V_{nk}\rho_{km} - \rho_{nk}V_{km}) - \gamma_{nm}(\rho_{nm} - \rho_{nm}^{(\mathrm{eq})}), \quad (2.32)$$

where $\omega_{nm} = E_{nm}/\hbar$, and we seek a solution

$$\rho_{nm} = \rho_{nm}^{(0)} + \lambda\rho_{nm}^{(1)} + \lambda^2\rho_{nm}^{(2)} + \cdots . \quad (2.33)$$

Turning the crank (see Ref. 10 for details) gives us the solution

$$\rho_{nm}^{(N)}(t) = \int_{-\infty}^{t} \frac{1}{i\hbar}[\lambda V(t'), \rho^{(N-1)}(t')]_{nm} e^{(i\omega_{nm}+\gamma_{nm})(t'-t)}\, dt'. \quad (2.34)$$

Carrying out this series to second order in λ with the perturbation $V(t) = -\boldsymbol{\mu}\cdot\boldsymbol{E}(t)$, where $\boldsymbol{\mu}$ is the dipole moment and $\boldsymbol{E}(t) = \sum_q \boldsymbol{E}(\omega_q)e^{-i\omega_q t}$ is the incident electric field, we get an expression for the density matrix $\rho_{nm}^{(2)}(t)$ as a function of the dipole matrix elements

$$\boldsymbol{\mu}_{nm} = \langle n|\, \boldsymbol{\mu}\, |m\rangle\,, \quad (2.35)$$

the frequencies ω_q, the damping constants γ_{nm}, and $\rho_{nm}^{(0)}$.

Once we have $\rho_{nm}^{(2)}(t)$, we can compute the expectation value

$$\langle\boldsymbol{\mu}(t)\rangle = \sum_{nm}\rho_{nm}(t)\boldsymbol{\mu}_{nm}, \quad (2.36)$$

from which the susceptibility can be computed by taking two derivatives with respect to the electric field amplitudes[8]. Reproducing the final an-

[8]We are specializing here to the case of electric dipole SHG, although the calculation proceeds similarly for magnetic dipole and electric quadrupole.

swer here (again, from Ref. 10):

$$\begin{aligned}\chi^{(2)}_{ijk}(\omega_p+\omega_q,\omega_q,\omega_p) = \frac{1}{2\epsilon_0\hbar^2}\sum_{lmn}(\rho^{(0)}_{ll}-\rho^{(0)}_{mm})\times\Big\{ \\ \frac{\mu^i_{ln}\mu^j_{nm}\mu^k_{ml}}{[(\omega_{nl}-\omega_p-\omega_q)-i\gamma_{nl}][(\omega_{ml}-\omega_p)-i\gamma_{ml}]} \\ +\frac{\mu^i_{ln}\mu^k_{nm}\mu^j_{ml}}{[(\omega_{nl}-\omega_p-\omega_q)-i\gamma_{nl}][(\omega_{ml}-\omega_q)-i\gamma_{ml}]} \\ +\frac{\mu^j_{ln}\mu^i_{nm}\mu^k_{ml}}{[(\omega_{nm}+\omega_p+\omega_q)+i\gamma_{nm}][(\omega_{ml}-\omega_p)-i\gamma_{ml}]} \\ +\frac{\mu^k_{ln}\mu^i_{nm}\mu^j_{ml}}{[(\omega_{nm}+\omega_p+\omega_q)+i\gamma_{nm}][(\omega_{ml}-\omega_q)-i\gamma_{ml}]} \\ \Big\},\end{aligned} \tag{2.37}$$

where $\omega_{nm} = \omega_n - \omega_m$. The SHG susceptibility tensor is then obtained by taking the limit $\omega_p = \omega_q$.

We learned two things by doing the quantum calculation. First of all, clearly if we know all of the eigenfunctions $|n\rangle$ of our unperturbed Hamiltonian, we can calculate the susceptibility tensor *a priori*, although this is obviously difficult except in the simplest of cases. Secondly, we notice that there are two types of denominators in eq. (2.37): those occuring at 2ω (remember we have set $\omega_q = \omega_p$) and those occuring at ω. Both can cause resonances in the SHG intensity and are observed abundantly in experiment [9]. The existence of resonances in the SHG spectrum makes comparison between different materials quite difficult if reference is made only to the SHG intensity at a single color. In one imfamous example, Wu *et al.* (Ref. 11) incorrectly attributed the large SHG amplitude at optical wavelengths in TaAs to the presence of Weyl nodes near the Fermi level; later SHG spectroscopy measurements demonstrated that the enhancement was due to a simple band resonance at the excitation frequency used in that paper [12]. The emerging consensus is that the SHG intensity at optical frequencies has more or less nothing to do with the low-energy excitation spectrum or its topology.

2.4 SHG in the Ginzburg-Landau paradigm

While eq. (2.37) is quite general and completely correct microscopically, it obviously lends very little intuition into what kind of phenomenology we can expect to find in the SHG signal, say, across a phase transition, where the dipole matrix elements which determine eq. (2.37) certainly change but may not do so in a simple or straightforward way. An alternative approach is to treat SHG in a generalized Ginzburg-Landau paradigm, in which all of the physics of the system is cast in terms of an order parameter $\mathscr{O}_{i_1 i_2 \ldots i_r}$. This approach was mainly developed by Sa *et al.* [**?**], based off of early work by Pershan [**?**] in the 1960s.

The key insight of Pershan is that one can define a "time-averaged free energy" in nonlinear optics by considering the term (assuming the incident field $E^{\text{in}}(t)$ is monochromatic with frequency ω)

$$F_{SHG} = -P_i(2\omega)E_i^{*\text{out}}(2\omega) + \text{c.c.} \tag{2.38}$$

$$= -[\chi_{ijk}E_i^{*\text{out}}(2\omega)E_j^{\text{in}}(\omega)E_k^{\text{in}}(\omega) + \text{c.c.}]. \tag{2.39}$$

Since F is a free energy, it must be a real, totally symmetric scalar, and eq. (2.39) thus gives us a way to *derive* the form of the tensor χ_{ijk} in a particular point group using similar arguments as in section 2.1.

In the context of a (spontaneous) symmetry-breaking transition at T_c, the Ginzburg Landau paradigm asserts that the free energy of eq. (2.39) still obeys the symmetry group of the high temperature phase, even though the low temperature phase explicitly breaks some of those symmetries. This is because the spontaneous symmetry breaking is considered a property of the *solution* of the free energy minimization problem, rather than a property of the minimization problem itself. Thus, a valid expression for the free energy in the low temperature phase is given by

$$F = -[\chi_{ijkl_1l_2\cdots l_r}(T > T_c)E_i^{*\text{out}}(2\omega)E_j^{\text{in}}(\omega)E_k^{\text{in}}(\omega) + \text{c.c.}]\mathscr{O}_{l_1l_2\cdots l_r}. \tag{2.40}$$

Comparing eqs. (2.39) and (2.40), we have an equation for the SHG susceptibility tensor in the low temperature phase

$$\chi_{ijk}(T < T_c) = \chi_{ijkl_1l_2\cdots l_r}(T > T_c)\mathscr{O}_{l_1l_2\cdots l_r}. \tag{2.41}$$

In light of eq. (2.41), let us consider the consequences of the symmetry of $\mathscr{O}$ on the SHG signal. For simplicity, let us consider a situation

that resembles a ferroelectric phase transition; i.e., the high temperature phase preserves inversion symmetry, but the low temperature phase involves the emergence of a rank-1 order parameter $\mathscr{O}_l$ which is odd under inversion. In that case, we have

$$\chi_{ijk}(T < T_c) = \chi_{ijkl}(T > T_c)\mathscr{O}_l(T), \tag{2.42}$$

i.e. the SHG at low temperature is simply a product of a high-temperature tensor and the order parameter $\mathscr{O}$. We of course need to check that χ_{ijkl} is allowed in the high temperature phase; here, we need χ_{ijkl} to be an even rank polar tensor, which is allowed in the presence of inversion symmetry (see eq. (2.10)).

Let us now imagine that the polarization $\mathscr{O}_l$ is known to be directed along the y axis, i.e.

$$\mathscr{O}_l = (0, P_0, 0)_l, \tag{2.43}$$

for some P_0. Then, by eq. (2.42), we have

$$\chi_{ijk}(T < T_c) = \chi_{ijky}(T > T_c)P_0. \tag{2.44}$$

Besides telling us that the susceptibility tensor is linear in the polarization magnitude P_0, what this formulation gets us is also that the elements of χ_{ijk} are just the elements of χ_{ijkl} with $l = y$. In many cases this is more information than you would have if you only knew the point group of the low temperature phase!

Equation (2.41) is also quite useful in the case where the low temperature phase is heterogenous; i.e. the order parameter $\mathscr{O}$ varies spatially from one point to another. This is commonly the case in magnets, for example, where rotational symmetry is spontaneously broken at T_c and the low temperature free energy thus consists of multiple energetically degenerate states related to each other by elements R of the high temperature point group which are broken at low temperature. These states have the same free energy since, again, the symmetry-breaking is due to to the order parameter, not due to the free energy itself. The order parameter in the different domains are thus related to each other via

$$\mathscr{O}_{i_1 i_2 \cdots i_r}(\boldsymbol{x}_1) = R[\mathscr{O}_{i_1 i_2 \cdots i_r}(\boldsymbol{x}_2)], \tag{2.45}$$

where the right hand side is given by eq. (2.10). Combining eq. (2.41) and eq. (2.45), the SHG tensor thus satisfies

$$\chi_{ijk}(\boldsymbol{x}_1) = R[\chi_{ijk}(\boldsymbol{x}_2)]. \tag{2.46}$$

Equation (2.46) is the fundamental basis for our SHG works on $1T$-TaS_2 and $CaMn_2Bi_2$, discussed in chapters **??** and **??**.

Chapter Three

Second harmonic generation: practical

In the last chapter we saw that the SHG intensity in a given crystal is related to the point group, order parameter, band structure, etc. of that crystal via the susceptibility tensor χ_{ijk}. It is also obvious from section 2.1 that the ideal scenario is to be able to measure as many of the numbers χ_{ijk} as possible; after all, if you only measured the xx component of eqs. (2.11) and (2.12), you would have obtained essentially no information about your crystal whatsoever. The SHG setup that we built (whose design is mostly credited to Torchinsky and Hsieh [**?**], with some improvements by us which I will discuss below) was designed with exactly this goal in mind. There are two key insights which make this design work: one, the light is obliquely incident on the sample so there is some component of $\boldsymbol{E}^{\text{in}}$ directed along the sample normal, and two, we rotate the plane of incidence so that the in-plane field direction sweeps an entire 360°. The first point allows us to measure elements of χ_{ijk} with z indices[1], and the second point makes sure we get all of the x and y elements of χ_{ijk} too. All of the tensor elements are thus given a chance to contribute to the SHG intensity in a given experiment.

With those considerations in mind, let me proceed to give a schematic description of our SHG setup. Some of the choices we made may seem arbitrary right now, but I will go over them in detail in **??**. The starting point is our regenerative amplifier (Spectra-Physics Spitfire Sptf-100f-5k-

[1]Here and unless otherwise noted I define the sample normal to be the z axis.

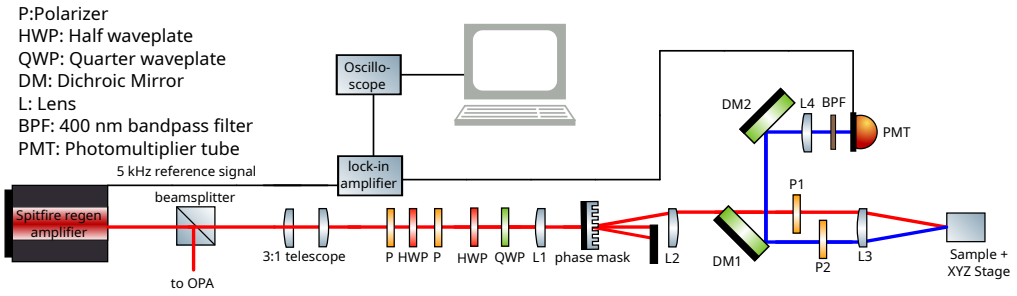

Figure 3.1: asdf

xp), which produces 100 fs 800 nm pulses at a 5 kHz repetition rate from an 86 MHz seed laser (Spectra-Physics Tsunami 3941-M1S). 90% of the beam is split off to power an optical parametric amplifier (OPA), and the remaining 10% is used for the SHG probe beam. After passing through an optical telescope, which creates a collimated beam of width $1-2$ mm, this beam is attenuated with a polarizer - half-wave plate - polarizer triplet, and then elliptically polarized with a quarter-wave plate and half-wave plate in series. The ellipticity at this stage is set so the light is perfectly circularly polarized following transmission through a phase mask, as described below.

After passing through these polarization optics, the beam is focused with a lens onto the aforementioned phase mask, which acts as a transmissive diffraction grating and separates the beam into multiple different diffraction orders. The $+1$ order diffraction comes off at an angle of roughly $7°$, while the other orders are blocked with anodized aluminum foil. This (diverging) beam then propogates at $7°$ to the optical axis before meeting a lens set at the appropriate distance so as to both collimate the beam and rectify the $7°$ progation angle. Then, the light passes through a dichroic mirror (which transmits 800 nm and reflects 400 nm), becomes linearly polarized by a wire-grid polarizer, and is then focused onto the sample at a $10°$ angle of incidence by passing through the edge of a 1 in-diameter 50 mm achromatic focusing lens. The interaction between the light and the sample causes SHG to be radiated in reflection at the same $10°$ angle of incidence, so that the SHG beam passes through the opposite side of the 50 mm lens before passing through a second, independent polarizer which is used to control the polarization of the measured light.

Finally, the polarized output reflects off of two dichroic mirrors (oriented in such a way as to cancel the differing effect of the Fresnel equations on the reflectivity of S and P polarized light) and is focused through a $400\ \mathrm{nm}$ bandpass filter onto a photomultiplier tube (PMT) by a $400\ \mathrm{mm}$ lens. The current output of the PMT is filtered by a lock-in amplifier (for static SHG, set to the $5\ \mathrm{kHz}$ repetition rate of the laser) and read out on an oscilloscope. The phase mask, incoming polarizer, and outgoing polarizer are mounted on rotating lens tubes which are connected via pulley to a common motor shaft driven by a brushless DC motor. The motor thus continuously rotates the plane of incidence of the experiment, since the latter is entirely defined by the phase mask and the polarizers. The rotation angle is tracked as a function of time by an optical rotary encoder, consisting of a laser pointer passed through a chopper wheel (with 100 slots) mounted at the end of the motor shaft and detected via photodiode. The encoder signal and the lock-in signal are both sent to a homemade oscilloscope (an Arduino Uno microcontroller which separates the lock-in signal into different individual rotations by looking for peaks in the encoder signal), the output of which is sent to a computer for further data processing.

Chapter Four

Second harmonic generation as a probe of broken mirror symmetry in 1T-TaS_2

Chapter Five

Light-induced reorientation transition in the antiferromagnetic semiconductor $CaMn_2Bi_2$

Chapter Six

Amplitude-mode electromagnon in the XXZ chain $CuBr_2$

Chapter Seven

Concluding remarks

*

Bibliography

[1] T. Kibble and G. Pickett, "Introduction. Cosmology meets condensed matter," *Phil. Trans. R. Soc. A.*, vol. 366, pp. 2793–2802, Aug. 2008.

[2] A. Alexandradinata, N. P. Armitage, A. Baydin, W. Bi, Y. Cao, H. J. Changlani, E. Chertkov, E. H. d. S. Neto, L. Delacretaz, I. E. Baggari, G. M. Ferguson, W. J. Gannon, S. A. A. Ghorashi, B. H. Goodge, O. Goulko, G. Grissonnanche, A. Hallas, I. M. Hayes, Y. He, E. W. Huang, A. Kogar, D. Kumah, J. Y. Lee, A. Legros, F. Mahmood, Y. Maximenko, N. Pellatz, H. Polshyn, T. Sarkar, A. Scheie, K. L. Seyler, Z. Shi, B. Skinner, L. Steinke, K. Thirunavukkuarasu, T. V. Trevisan, M. Vogl, P. A. Volkov, Y. Wang, Y. Wang, D. Wei, K. Wei, S. Yang, X. Zhang, Y.-H. Zhang, L. Zhao, and A. Zong, "The Future of the Correlated Electron Problem," July 2022.
arXiv:2010.00584 [cond-mat].

[3] F. Neumann, *Vorlesungen über die Theorie der Elasticität der festen Körper und des Lichtäthers, gehalten an der Universität Königsberg*.
Leipzig, B. G. Teubner, 1885.

[4] P. Curie, "Sur la symétrie dans les phénomènes physiques, symétrie d'un champ électrique et d'un champ magnétiqueu," *J. Phys. Theor. Appl.*, vol. 3, no. 1, pp. 393–415, 1894.

[5] Wikipedia contributors, "List of space groups — Wikipedia, the free encyclopedia," 2024.
[Online; accessed 06-March-2024].

[6] R. C. Powell, *Symmetry, Group Theory, and the Physical Properties of Crystals*.
Springer New York, NY, 2010.

[7] R. R. Birss, *Symmetry and Magnetism*.
North-Holland Pub. Co., 1964.

[8] J. D. Jackson, *Classical electrodynamics*.
New York, NY: Wiley, 3rd ed. ed., 1999.

[9] M. Fiebig, D. Fröhlich, T. Lottermoser, V. V. Pavlov, R. V. Pisarev, and H.-J. Weber, "Second Harmonic Generation in the Centrosymmetric Antiferromagnet NiO," *Phys. Rev. Lett.*, vol. 87, p. 137202, Sept. 2001.

[10] R. Boyd, *Nonlinear Optics*.
Academic Press, third ed., mar 2008.

[11] L. Wu, S. Patankar, T. Morimoto, N. L. Nair, E. Thewalt, A. Little, J. G. Analytis, J. E. Moore, and J. Orenstein, "Giant anisotropic nonlinear optical response in transition metal monopnictide Weyl semimetals," *Nature Phys*, vol. 13, pp. 350–355, Apr. 2017.

[12] S. Patankar, L. Wu, B. Lu, M. Rai, J. D. Tran, T. Morimoto, D. E. Parker, A. G. Grushin, N. L. Nair, J. G. Analytis, J. E. Moore, J. Orenstein, and D. H. Torchinsky, "Resonance-enhanced optical nonlinearity in the Weyl semimetal TaAs," *Phys. Rev. B*, vol. 98, p. 165113, Oct. 2018.